

Relating parton model and color dipole formulation of heavy quark hadroproduction

Jörg Raufeisen^a and Jen-Chieh Peng^b

^a *Los Alamos National Laboratory, MS H846, Los Alamos, NM 87545, USA*

^b *Department of Physics, University of Illinois, Urbana, IL 61801, USA*

Abstract

At high center of mass energies, hadroproduction of heavy quarks can be expressed in terms of the same color dipole cross section as low Bjorken- x deep inelastic scattering. We show analytically that at leading order, the dipole formulation is equivalent to the gluon-gluon fusion mechanism of the conventional parton model. In phenomenological application, we employ a parameterization of the dipole cross section which also includes higher order and saturation effects, thereby going beyond the parton model. Numerical calculations in the dipole approach agree well with experimental data on open charm production over a wide range of energy. Dipole approach and next to leading order parton model yield similar values for open charm production, but for open bottom production, the dipole approach tends to predict somewhat higher cross sections than the parton model.

PACS: 13.85.Ni

Keywords: Heavy Quarks; Dipole Cross Section

I. INTRODUCTION

Heavy quark hadroproduction has been conventionally described in the framework of QCD parton model [1, 2, 3]. At high center of mass energies \sqrt{s} , many hard-processes, including Drell-Yan [4] and heavy-quark production [5, 6], can be described in terms of the color dipole cross sections originally deduced from low x_{Bj} deep inelastic scattering (DIS) (see *e.g.* [7]). The dipole formulation of heavy quark production was first introduced in [5]. This alternative approach to heavy quark production provides a theoretical framework for treating the nuclear effects, which are present in high energy proton-nucleus and nucleus-nucleus collisions. However, the connection between this dipole approach and the conventional parton model approach remains to be delineated and clarified. The purpose of this paper is to demonstrate the validity of the dipole approach in proton-proton (pp) collisions and to illuminate its relation to the conventional parton model.

An alternative approach to heavy quark production that is designed especially for energies much larger than the heavy quark mass m_Q and which is able to describe nuclear effects is desirable for a variety of reasons. At low x , the heavy quark pair is produced over large longitudinal distances, which can exceed the radius of a large nucleus by orders of magnitude. Indeed, even though the matrix element of a hard process is dominated by short distances, of the order of the inverse of the hard scale, the cross section of that process also depends on the phase space element. Due to gluon radiation, the latter becomes very large at high energies, and it is still a challenge how to resum the corresponding low- x logarithms. The dipole formulation allows for a simple phenomenological recipe to include these low- x logs. The large length scale in the problem leads to pronounced nuclear effects, giving one the possibility to use nuclear targets as microscopic detectors to study the space-time evolution of heavy quark production.

In addition, heavy quark production is of particular interest, because this process directly probes the gluon distributions of the colliding particles. Note that at the tremendous center of mass energies of the Relativistic Heavy Ion Collider (RHIC) and especially of the Large Hadron Collider (LHC), charm (and at LHC also bottom) decays will dominate the dilepton continuum [8]. Thus, a measurement of the heavy quark production cross section at RHIC and LHC will be relatively easy to accomplish and can yield invaluable information about the (nuclear) gluon density [9]. It is expected that at very low x , the growth of the gluon density

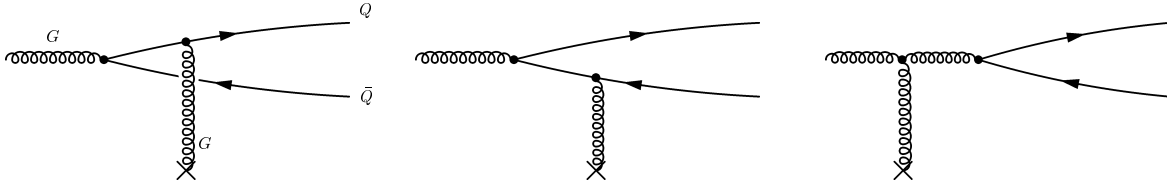


FIG. 1: *The three lowest order graphs contributing to heavy quark production in the dipole approach. These graphs correspond to the gluon-gluon fusion mechanism of heavy quark production in the parton model.*

will be slowed down by nonlinear terms in the QCD evolution equations [10]. The onset of this non-linear regime is controlled by the so-called saturation scale $Q_s(x, A)$, which is already of order of the charm quark mass at RHIC and LHC energies. Moreover, $Q_s(x, A) \propto A^{1/3}$ (A is the atomic mass of the nucleus), so that one can expect sizable higher twist corrections in AA collisions [6]. Note that saturation will lead to a breakdown of the twist expansion, since one cannot conclude any more that terms suppressed by powers of the heavy quark mass m_Q are small, $Q_s^n(x, A)/m_Q^n \in O(1)$ for any n . Saturation effects are most naturally described in the dipole picture.

II. COLOR DIPOLE APPROACH TO HEAVY QUARK HADROPRODUCTION

The color dipole approach is formulated in the target rest frame, where heavy quark production looks like pair creation in the target color field, Fig. 1. For a short time, a gluon G from the projectile hadron can develop a fluctuation which contains a heavy quark pair ($Q\bar{Q}$). Interaction with the color field of the target then may release these heavy quarks. The similarity between heavy quark production and pair creation at high partonic center of mass energies has already been pointed out in [1]. Apparently, the mechanism depicted in Fig. 1 corresponds to the gluon-gluon fusion mechanism of heavy quark production in the leading order (LO) parton model. The dipole formulation is therefore applicable only at low x_2 , where the gluon density of the target is much larger than all quark densities[30]. The kinematical range where the dipole approach is valid can of course only be determined a posteriori. This is similar to determining the minimal value of Q^2 for which perturbative QCD still works.

We will now present formulae for the partonic cross section for producing a heavy quark

pair $Q\bar{Q}$, limiting ourselves to presenting only the final result. The production amplitudes can be found in [6]. The derivation can be performed along the same lines as for Drell-Yan, which is explained in detail in the appendix of [11].

After summation over all three color states in which the $Q\bar{Q}$ pair in Fig. 1 can be produced, one obtains for the partonic cross section [6],

$$\sigma(GN \rightarrow \{Q\bar{Q}\}X) = \int_0^1 d\alpha \int d^2\rho |\Psi_{G \rightarrow Q\bar{Q}}(\alpha, \rho)|^2 \sigma_{q\bar{q}G}(\alpha, \rho), \quad (1)$$

where $\sigma_{q\bar{q}G}$ is the cross section for scattering a color neutral quark-antiquark-gluon system on a nucleon [6],

$$\sigma_{q\bar{q}G}(\alpha, \rho) = \frac{9}{8} [\sigma_{q\bar{q}}(\alpha\rho) + \sigma_{q\bar{q}}(\bar{\alpha}\rho)] - \frac{1}{8}\sigma_{q\bar{q}}(\rho). \quad (2)$$

Here α is the light-cone momentum fraction carried by the heavy quark Q , and $\bar{\alpha}$ is the momentum fraction of the \bar{Q} . In LO, with no additional gluon in the final state, $\alpha + \bar{\alpha} = 1$. The dipole cross section $\sigma_{q\bar{q}}(\rho)$ is an eigenvalue of the forward diffraction amplitude operator and has to be determined from experimental data. It depends on the transverse separation ρ between quark and antiquark. We point out that $\sigma_{q\bar{q}}(\rho)$ is flavor independent, *i.e.* it is the same for a dipole of heavy quarks ($Q\bar{Q}$) as for light quarks ($q\bar{q}$). Note that the dipole cross section would be independent of energy, if only the Born graphs in Fig. 1 were taken into account. However, higher order corrections will make $\sigma_{q\bar{q}}$ a function x_2 . In order to simplify the notation, we do not explicitly write out the x_2 dependence of the dipole cross section.

The light-cone (LC) wavefunctions for the transition $G \rightarrow Q\bar{Q}$ can be calculated perturbatively,

$$\begin{aligned} \Psi_{G \rightarrow Q\bar{Q}}(\alpha, \vec{\rho}_1) \Psi_{G \rightarrow Q\bar{Q}}^*(\alpha, \vec{\rho}_2) = & \frac{\alpha_s(\mu_R)}{(2\pi)^2} \left\{ m_Q^2 K_0(m_Q \rho_1) K_0(m_Q \rho_2) \right. \\ & \left. + [\alpha^2 + \bar{\alpha}^2] m_Q^2 \frac{\vec{\rho}_1 \cdot \vec{\rho}_2}{\rho_1 \rho_2} K_1(m_Q \rho_1) K_1(m_Q \rho_2) \right\}, \end{aligned} \quad (3)$$

where $\alpha_s(\mu_R)$ is the strong coupling constant, which is probed at a renormalization scale $\mu_R \sim m_Q$. We work in a mixed representation, where the longitudinal direction is treated in momentum space, while the transverse directions are described in coordinate space representation.

Partonic configurations with fixed transverse separations in impact parameter space have been identified as eigenstates of the interaction a long time ago [12, 13]. Since the degrees of freedom in the dipole approach are eigenstates of the interaction, this approach is especially suitable to describe multiple scattering effects, *i.e.* nuclear effects [5, 6].

Eq. (1) is a special case of the general rule that at high energy, the cross section for the reaction $a + N \rightarrow \{b, c, \dots\}X$ can be expressed as convolution of the LC wavefunction for the transition $a \rightarrow \{b, c, \dots\}$ and the cross section for scattering the color neutral $\{\text{anti-}a, b, c, \dots\}$ -system on the target nucleon N .

Note that although the dipole cross section is flavor independent, the integral Eq. (1) is not. Since the Bessel functions $K_{1,0}$ decay exponentially for large arguments, the largest values of ρ which can contribute to the integral are of order $\sim 1/m_Q$. We point out, that as a consequence of color transparency [12, 14], the dipole cross section vanishes $\propto \rho^2$ for small ρ . Therefore, the $Q\bar{Q}$ production cross section behaves roughly like $\propto 1/m_Q^2$ (modulo logs and saturation effects).

In order to calculate the cross section for heavy quark pair production in pp collisions, Eq. (1) has to be weighted with the projectile gluon density,

$$\frac{d\sigma(pp \rightarrow \{Q\bar{Q}\}X)}{dy} = x_1 G(x_1, \mu_F) \sigma(GN \rightarrow \{Q\bar{Q}\}X), \quad (4)$$

where $y = \frac{1}{2} \ln(x_1/x_2)$ is the rapidity of the pair and $\mu_F \sim m_Q$. In analogy to the parton model, we call μ_F the factorization scale. Uncertainties arising from the choice of this scale will be investigated in section III. Integrating over all kinematically allowed rapidities yields

$$\sigma_{\text{tot}}(pp \rightarrow \{Q\bar{Q}\}X) = 2 \int_0^{-\ln(\frac{2m_Q}{\sqrt{s}})} dy x_1 G(x_1, \mu_F) \sigma(GN \rightarrow \{Q\bar{Q}\}X). \quad (5)$$

A word of caution is in order, regarding the limits of the α -integration in Eq. (1). Since the invariant mass of the $Q\bar{Q}$ -pair is given by

$$M_{Q\bar{Q}}^2 = \frac{k_\perp^2 + m_Q^2}{\alpha\bar{\alpha}}, \quad (6)$$

the endpoints of the α -integration include configurations corresponding to arbitrarily large invariant masses, eventually exceeding the total available $cm.$ energy. However, since ρ and k_\perp (the single quark transverse momentum) are conjugate variables, the pair mass is not defined in the mixed representation, nor are the integration limits for α . Fortunately, this problem is present only at the very edge of the phase space and therefore numerically negligible.

Because of the mixed representation, in which the invariant mass of the pair is not defined, the formulae for the $M_{Q\bar{Q}}$ distributions will be somewhat more complicated. In a first step,

we present a formula for the single quark k_\perp distributions, which can be obtained after a simple calculation from the amplitudes given in section 2.1 of [6]. One finds,

$$\begin{aligned} \frac{d^3\sigma(GN \rightarrow \{Q\bar{Q}\}X)}{d^2k_\perp d\alpha} &= \frac{1}{(2\pi)^2} \int d^2\rho_1 d^2\rho_2 e^{i\vec{k}_\perp \cdot (\vec{\rho}_1 - \vec{\rho}_2)} \Psi_{G \rightarrow Q\bar{Q}}(\alpha, \vec{\rho}_1) \Psi_{G \rightarrow Q\bar{Q}}^*(\alpha, \vec{\rho}_2) \\ &\times \frac{1}{2} \left\{ \frac{9}{8} [\sigma_{q\bar{q}}(\alpha\rho_1) + \sigma_{q\bar{q}}(\bar{\alpha}\rho_1) + \sigma_{q\bar{q}}(\alpha\rho_2) + \sigma_{q\bar{q}}(\bar{\alpha}\rho_2)] \right. \\ &\quad - \frac{1}{8} [\sigma_{q\bar{q}}(\alpha\vec{\rho}_1 + \bar{\alpha}\vec{\rho}_2) + \sigma_{q\bar{q}}(\bar{\alpha}\vec{\rho}_1 + \alpha\vec{\rho}_2)] \\ &\quad \left. - [\sigma_{q\bar{q}}(\alpha|\vec{\rho}_1 - \vec{\rho}_2|) + \sigma_{q\bar{q}}(\bar{\alpha}|\vec{\rho}_1 - \vec{\rho}_2|)] \right\}. \end{aligned} \quad (7)$$

After integration over k_\perp , one obviously recovers Eq. (1).

The heavy quark pair invariant mass distribution is now easily obtained,

$$\frac{d\sigma(pp \rightarrow \{Q\bar{Q}\}X)}{dM_{Q\bar{Q}}^2} = 2 \int_0^{-\ln(\sqrt{\tau})} dy x_1 G(x_1, \mu_F) \int_{\alpha_{min}}^{\alpha_{max}} d\alpha \alpha \bar{\alpha} \pi \frac{d^3\sigma(GN \rightarrow \{Q\bar{Q}\}X)}{d^2k_\perp d\alpha}, \quad (8)$$

where $\tau = M_{Q\bar{Q}}^2/s$, and the limits of the α -integration now depend on $M_{Q\bar{Q}}$,

$$\alpha_{max/min} = \frac{1}{2} (1 \pm \sqrt{1-v}), \quad (9)$$

$$v = \frac{4m_Q^2}{M_{Q\bar{Q}}^2}. \quad (10)$$

It is possible to retrieve from Eq. (8) the corresponding leading order parton model formula. Note that in leading order and for small separations ρ , the dipole cross section can be expressed in terms of the target gluon density [15],

$$\sigma_{q\bar{q}}(x, \rho) = \frac{\pi^2}{3} \rho^2 \alpha_s(\mu) x G(x, \mu). \quad (11)$$

In DIS, μ in Eq. (11) is given by $\mu = \lambda/\rho$ where λ is a number, since this is the only available dimensionful scale at which the gluon density could be probed. However, in the case of heavy quark production, it seems plausible that μ is of order of m_Q , *i.e.* $\mu = \mu_{R,F}$. Then, the curly bracket in Eq. (7) reduces to

$$\left\{ \dots \right\}_{Eq. (7)} = \frac{\pi^2}{3} \alpha_s(\mu_R) x G(x, \mu_F) 2\vec{\rho}_1 \cdot \vec{\rho}_2 \left(\alpha^2 - \frac{\alpha\bar{\alpha}}{4} + \bar{\alpha}^2 \right), \quad (12)$$

and it is possible to perform all but the y -integral in Eq. (8) analytically. The result is

$$\begin{aligned} \frac{d\sigma(pp \rightarrow \{Q\bar{Q}\}X)}{dM_{Q\bar{Q}}^2} &= \alpha_s^2(\mu_R) 2 \int_0^{-\ln(\sqrt{\tau})} dy x_1 G(x_1, \mu_F) x_2 G(x_2, \mu_F) \\ &\times \frac{\pi}{192M_{Q\bar{Q}}^4} \left\{ (v^2 + 16v + 16) \ln\left(\frac{1+\beta}{1-\beta}\right) - 28\beta - 31v\beta \right\}, \end{aligned} \quad (13)$$

where $\beta = \sqrt{1-v}$. Changing the integration variables to x_1 and x_2 , we obtain for the total cross section,

$$\begin{aligned} \sigma_{\text{tot}}(pp \rightarrow \{Q\bar{Q}\}X) &= \frac{\alpha_s^2(\mu_R)}{m_Q^2} \int dx_1 dx_2 G(x_1, \mu_F) G(x_2, \mu_F) \\ &\times \frac{\pi v}{192} \left\{ (v^2 + 16v + 16) \ln\left(\frac{1+\beta}{1-\beta}\right) - 28\beta - 31v\beta \right\}. \end{aligned} \quad (14)$$

Note that Eq. (14) exactly agrees with the LO parton model result for the gluon-gluon contribution to the heavy quark production cross section (see Eqs. (7,8,10,15) in [1]). Thus, we have shown that in leading order α_s and in leading twist approximation, dipole approach and parton model become equivalent at high energies, when the gluon-gluon contribution in the parton model dominates. Furthermore, in leading-log x_2 approximation, the dipole cross section in the formulae for heavy quark production is the same as in DIS, and is given by Eq. (11). Note that Eqs. (4) and (5) are not analytically equivalent to their parton model counterparts because of the inaccuracy in the α -integration.

A calculation of higher order corrections is beyond the scope of this paper. Nevertheless, higher order corrections are important, because they provide a mechanism for the generation of large transverse momenta of the heavy quark pair. It would also be interesting to see, if the relation between $\sigma_{q\bar{q}}$ and $\sigma_{q\bar{q}G}$, Eq. (2), persists to higher orders. It is possible to calculate higher order corrections systematically in the dipole approach. This has been done in the case of DIS in the generalized BFKL approach of Nikolaev and Zakharov, see *e.g.* [7]. However, the widely discussed next-to-leading order (NLO) correction to the BFKL equation [16], has left the theory of low- x resummation in an unclear state. We conclude this section with the remark that, whatever the result of a higher order calculation will be, it will not be possible to reproduce the complete NLO correction of the parton model [1, 2, 3] in the dipole approach. Only terms enhanced by a factor $\log(x_2)$ can be reproduced. This limitation is inherent to the dipole formulation.

III. PHENOMENOLOGICAL APPLICATIONS

Now that it has been shown that the dipole formulation and the conventional parton model are equivalent in a certain approximation, still the questions remain, how well does the dipole approach describe experimental data, and how much do predictions from both approaches differ from each other. Note that we do not use the leading order gluon density to

calculate the dipole cross section according to Eq. (11), instead we employ the phenomenological parameterization of [17] for $\sigma_{q\bar{q}}$, which reduces to Eq. (11) in the limit $\rho \rightarrow 0$ and includes saturation effects at larger transverse separations. This parameterization is an improved version of the saturation model presented in [18], which now also includes DGLAP evolution. We use fit 1 of [17], since the non-monotonous behavior of fit 2 as a function of ρ seems unphysical to us. Both fits are constrained by HERA DIS data for $x_{Bj} \leq 0.01$.

We stress that $\sigma_{q\bar{q}}(x_2, \rho)$ contains much more information than the ordinary parameterizations of the gluon density. The unintegrated gluon density is related to the dipole cross section by Fourier transform (see *e.g.* [17, 18]). Thus, $\sigma_{q\bar{q}}(x_2, \rho)$ also contains information about the transverse momentum distribution of low- x gluons in a nucleon. The x_2 dependence and the intrinsic transverse momentum parameterized in the dipole cross section are higher order effects, which are taken into account in the dipole approach in this phenomenological way. Therefore, we compare predictions of the dipole approach for open charm and bottom production to NLO parton model calculation. The latter were performed with the code of [1, 2, 3], using GRV98HO parton distributions [19] in $\overline{\text{MS}}$ scheme.

In the dipole approach, we use the one loop running coupling constant,

$$\alpha_s(\mu_R) = \frac{4\pi}{\left(11 - \frac{2}{3}N_f\right) \ln\left(\frac{\mu_R^2}{(200 \text{ MeV})^2}\right)} \quad (15)$$

at a renormalization scale $\mu_R \sim m_Q$, and the number of light flavors is chosen to be $N_f = 3$ for open charm and $N_f = 4$ for open bottom production. Furthermore, we use the GRV98LO [19] gluon distribution (from CERNLIB [20]) to model the gluon density in the projectile. We use a leading order parton distribution function (PDF), because of its probabilistic interpretation. Note that one could attempt to calculate the projectile gluon distribution from the dipole cross section. However, the projectile distribution functions are needed mostly at large momentum fraction x_1 , where the dipole cross section is not constrained by data.

Our results for the total charm pair cross section in proton-proton (pp) collisions is shown in Fig. 2 as function of center of mass energy. The left panel shows the uncertainties of both approaches by varying quark mass m_c and renormalization scale μ_R in the intervals $1.2 \text{ GeV} \leq m_c \leq 1.8 \text{ GeV}$ and $m_c \leq \mu_R \leq 2m_c$, respectively. The factorization scale is kept fixed at $\mu_F = 2m_c$, because in our opinion, the charm quark mass is too low for DGLAP evolution. A large fraction of the resulting uncertainty originates from different possible

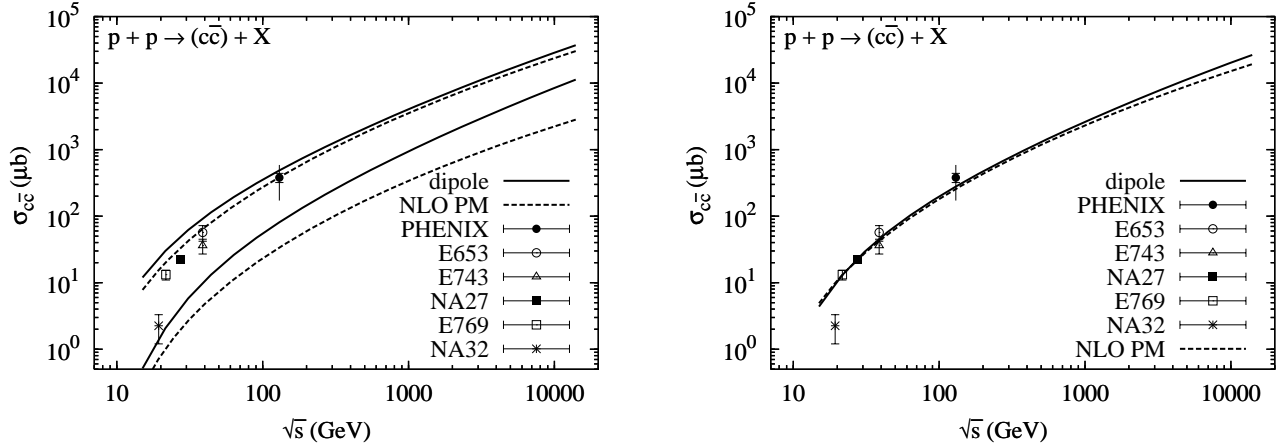


FIG. 2: Results for the total open charm pair cross section as function of \sqrt{s} . Varying free parameters in dipole approach (solid lines) and in the parton model (dashed lines) gives rise to the uncertainties shown on the left. In the figure on the right, parameters in both models have been adjusted so that experimental data are described.

choices of the charm quark mass, since the total cross section behaves approximately like $\sigma_{\text{tot}} \propto m_Q^{-2}$.

Note that the mean value of x_2 increases with decreasing energy. At $\sqrt{s} = 130$ GeV one has $x_2 \sim 0.01$. For lower energies, our calculation is an extrapolation of the saturation model. For the highest fixed target energies of $\sqrt{s} \approx 40$ GeV, values of $x_2 \sim 0.1$ become important. Unlike in the Drell-Yan case, which was studied in [11], the dipole approach to heavy quark production does not show any unphysical behavior when extrapolated to larger x_2 . One reason for this is that the new saturation model [17] assumes a realistic behavior of the gluon density at large x_2 . In addition, even at energies as low as $\sqrt{s} = 15$ GeV, the gluon-gluon fusion process is the dominant contribution to the cross section.

Because of the wide uncertainty bands, one can adjust m_c and μ_R in both approaches so that experimental data are reproduced. Then, dipole approach and NLO parton model yield almost identical results. However, the predictive power of the theory is rather small. In Fig. 2 (right), we used $m_c = 1.2$ GeV and $\mu_R = 1.5m_c$ for the NLO parton model calculation and $m_c = 1.4$ GeV, $\mu_R = m_c$ in the dipole approach. The data points tend to lie at the upper edge of the uncertainty bands, so that rather small values of m_c are needed to describe them.

There are remaining uncertainties which are not shown in Fig. 2 (right), because different

combinations of m_c and μ_R can also yield a good description of the data. In addition, different PDFs will lead to different values of the cross section at high energies, since the heavy quark cross section is very sensitive to the low- x gluon distribution. In [21], it was found that an uncertainty of a factor of ~ 2.3 remains at $\sqrt{s} = 14$ TeV (in the NLO parton model), even after all free parameters had been fixed to describe total cross section data at lower energies. In the dipole approach, the low- x gluon distribution of the target is modeled by the dipole cross section. Since there are not many successful parameterizations of $\sigma_{q\bar{q}}$, it is difficult to quantify the uncertainty resulting from this quantity. Using the old saturation model [18] instead of the DGLAP improved one [17] leads only to small differences for open charm production (this is not the case for bottom production, see below). However, it is reasonable to expect that the uncertainty will be at least as large as in the parton model, *i.e.* a factor of 2.3. Therefore, it will probably be impossible to find any signs of saturation in the total cross section for open charm production. It is however interesting to see that 20 – 30% of the total pp cross section at LHC ($\sqrt{s} = 14$ TeV) goes into open charm [31].

A few remarks are in order concerning the data shown in Fig. 2. The fixed target data [23] (*i.e.* all points except the one from PHENIX [24]) were taken in proton-nucleon collisions, and the quantity that was actually measured was the D -meson cross section for Feynman $x_F > 0$. We corrected the data for the contribution to open charm from charmed baryons and for the partial x_F coverage according to the prescription of [25]. The PHENIX point was measured in $AuAu$ collisions, assuming that there is no contribution to the single electron signal from sources unrelated to charm production, such as thermal direct photons or thermal di-leptons. The data point shown in the figure is for central collisions. We did not correct for nuclear (anti-)shadowing effects, either.

Next, we calculate the total $b\bar{b}$ -pair cross section as function of center of mass energy, see Fig. 3. In order to quantify the theoretical uncertainties, we vary the free parameters over the ranges $4.5 \text{ GeV} \leq m_b \leq 5 \text{ GeV}$ and $m_b \leq \mu_R, \mu_F \leq 2m_b$. Because of the large b -quark mass, uncertainties are much smaller than for open charm production. One can see that the dipole approach tends to predict higher values than the NLO parton model, even though the energy dependence expected in both approaches is very similar. In fact, the results calculated in the dipole approach with $m_b = 5 \text{ GeV}$ agree almost exactly with the NLO parton model calculation with $m_b = 4.5 \text{ GeV}$. For all other values of m_b , the uncertainty bands of the two approaches do not overlap, in contrast to the case for open

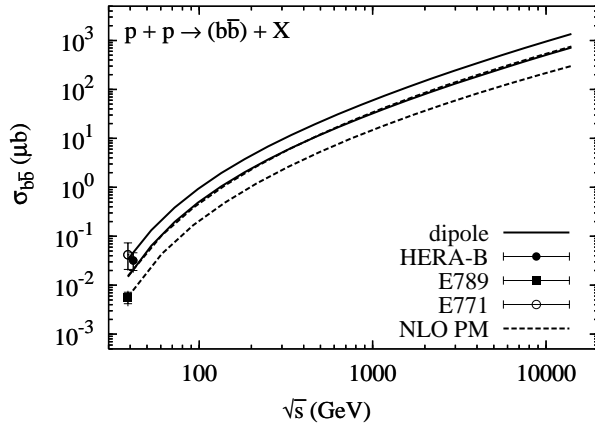


FIG. 3: *Uncertainties of open $b\bar{b}$ pair production calculated in the dipole approach (solid) and in the NLO parton model (dashed). The dipole approach seems to provide a better description of the data, even though HERA-B energy is too low for the dipole approach.*

charm production.

Three measurements of open $b\bar{b}$ production are published in the literature [26, 27, 28]. The two values of the open bottom cross section measured at Fermilab [26, 27] at $cm.$ energy $\sqrt{s} = 38.8 \text{ GeV}$ differ by almost three standard deviations. The HERA-B measurement at slightly larger $cm.$ energy $\sqrt{s} = 41.6 \text{ GeV}$ [28] is consistent with the E771 [27] value. These two points seem to be better described by the dipole approach, though the NLO parton model (with $m_b = 4.5 \text{ GeV}$) still touches the HERA-B error bar. Note that also a different set of PDFs would not significantly pull up the parton model curve [21], as a lower value of the b -quark mass would do. With a resummation of terms from higher order corrections [29], however, the parton model can reproduce each of the three measurements within theoretical uncertainties, see [28]. On the other hand, typical values of x_2 which are important for $b\bar{b}$ production at HERA-B energy are of order $x_2 \sim 0.2$, while the parameterization [17] of the dipole cross section is constrained only by DIS data with $x_{Bj} \leq 0.01$.

We point out that it is essential to use the DGLAP improved saturation model of [17] in order to obtain the same energy dependence in the dipole approach as in the NLO parton model. The older saturation model of [18] predicts a much weaker energy dependence.

Finally, we calculate the rapidity distribution of heavy quark pairs, Fig. 4. For open charm production, we use the values of m_c , μ_F and μ_R that describe the total cross section data. With this choice, the rapidity distributions expected in both approaches are very similar in shape and absolute normalization. The single PHENIX point has large errorbars, but is nevertheless well described by both approaches. The curves for $b\bar{b}$ production (Fig. 4) in the dipole approach are calculated with $m_b = \mu_F = \mu_R = 4.9 \text{ GeV}$, because this set

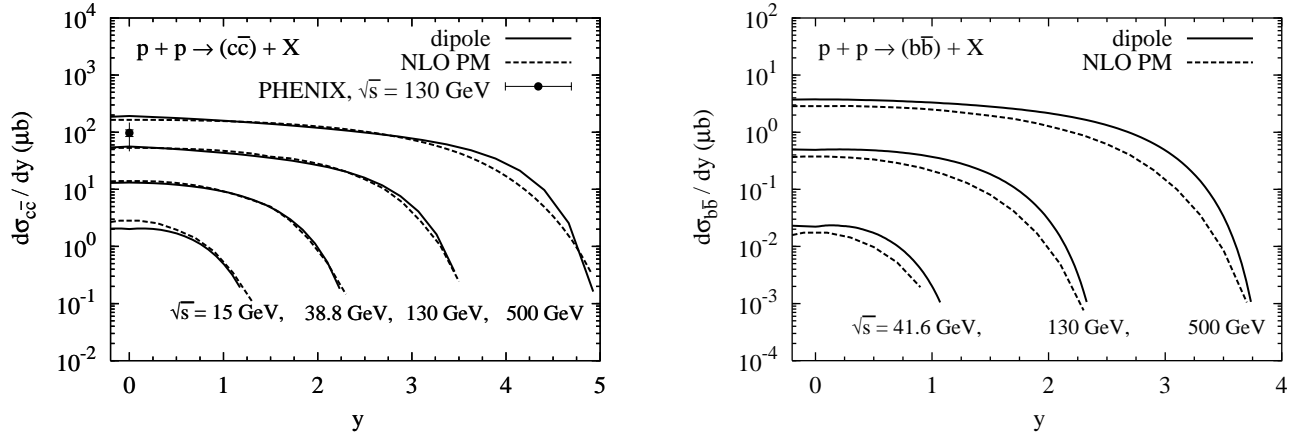


FIG. 4: Rapidity distribution of heavy quark pairs. In the case of open charm (left) free parameters of both approaches were chosen such that total cross section data are described i.e. as in Fig. 2 (left). The same was done for $b\bar{b}$ production (right) in the dipole approach (solid curves). In the NLO parton model (dashed curves), we used the parameter set that yielded the largest cross section.

of parameter values describes well the HERA-B point. The parton model calculation was performed with $m_b = \mu_R = 4.5 \text{ GeV}$ and $\mu_F = 2m_b$. This combination yields the upper parton model curve in Fig. 3. Even though the shape of the rapidity distributions in the two approaches are similar, somewhat larger cross sections are expected in the dipole approach. We have checked that the rapidity integral over the parton model curves in Fig. 4 reproduces the total cross sections shown in Figs. 2 and 3.

While it is an advantage of the dipole formulation to provide very simple formulas that allow one to absorb much of the higher order corrections into a phenomenological parameterization of $\sigma_{q\bar{q}}(x_2, \rho)$, one cannot clarify the origin of the discrepancy in normalizations without a systematic calculation of higher orders in this approach. Such a calculation is in principle possible, but is beyond the scope of this paper.

IV. SUMMARY AND OUTLOOK

In this paper, we employed the color dipole approach to study heavy quark pair production in pp collisions. We analytically related the leading order dipole approach to the lowest order parton model, thereby putting the dipole formulation on a more firm theoretical

basis. In phenomenological applications to the total heavy quark pair cross section and the pair rapidity distribution, large theoretical uncertainties arise, mostly from different possible choices of the heavy quark mass. This is especially true for open charm production. Nevertheless, experimental data can be described in the dipole approach with realistic parameter values. In kinematical regions where no data are available, predictions from the dipole approach and the NLO parton model for open charm production agree well after all free parameters are fixed to describe the existing data. Note that we employ a phenomenological parameterization of the dipole cross section, which is supposed to include higher order effects as well, so that there is no justification for introducing an arbitrary overall normalization factor (“ K -factor”).

Theoretical uncertainties in the cross section value, which arise from the heavy quark mass are much smaller in the case of open b -production. In this case, predictions from the dipole approach tend to be higher than the NLO parton model, but the curves are similar in shape (provided QCD evolution is included in the dipole approach). Even though two out of three fixed target measurements of $b\bar{b}$ -production seem to be better described by the dipole approach, one has to bear in mind that fixed target energies are too low for a reliable application of the dipole approach. Future experimental data at higher energies will show, whether the dipole approach can reproduce the correct normalization of the cross section.

A special advantage of the dipole formulation is the simplicity of its formulae, which allow one to calculate the rapidity distribution of heavy quark pairs in only a few seconds. In addition, it is particularly easy to calculate nuclear effects in heavy quark production within this formulation [5, 6]. In fact, the latter point has been the original motivation for developing this approach.

In the future, it will be necessary to systematically calculate higher order correction in the dipole approach, in order to find out which part of these corrections can be taken into account by a phenomenological parameterization of the dipole cross section. This is especially important in view of the transverse momentum distribution of heavy quark pairs. In the dipole approach as presented in this paper, all transverse momentum of the pair can originate only from the intrinsic transverse momentum of the target gluon, which is encoded in the dipole cross section. This intrinsic transverse momentum should not be confused with the primordial p_T which is sometimes introduced in phenomenological approaches. Part of the intrinsic p_T parameterized in the dipole cross section originates from higher orders in

perturbation theory. An investigation of higher order corrections will also help clarifying the origin of the different absolute normalizations of dipole approach and parton model for open b -production. In addition, a good theoretical understanding of the transverse momentum dependence of heavy quark production in the dipole formulation should be achieved before one applies this approach to describe Tevatron measurements. We finally mention that single inclusive hadroproduction of heavy quarks can be formulated in the dipole approach as well. We shall address these topics in a future publication.

Acknowledgments: J.R. is indebted to Boris Kopeliovich for valuable discussion. This work was supported by the U.S. Department of Energy at Los Alamos National Laboratory under Contract No. W-7405-ENG-38.

-
- [1] P. Nason, S. Dawson and R. K. Ellis, Nucl. Phys. B **303**, 607 (1988).
 - [2] P. Nason, S. Dawson and R. K. Ellis, Nucl. Phys. B **327**, 49 (1989) [Erratum-ibid. B **335**, 260 (1990)].
 - [3] M. L. Mangano, P. Nason and G. Ridolfi, Nucl. Phys. B **373**, 295 (1992). A FORTRAN code for the NLO calculation is available at <http://n.home.cern.ch/n/nason/www/hvqlib.html>.
 - [4] B. Z. Kopeliovich, proc. of the workshop *Dynamical Properties of Hadrons in Nuclear Matter*, Hirschegg, January 16 – 21, 1995, ed. by H. Feldmeyer and W. Nörenberg, Darmstadt, 1995, p. 102 (hep-ph/9609385);
S. J. Brodsky, A. Hebecker and E. Quack, Phys. Rev. D **55**, 2584 (1997) [arXiv:hep-ph/9609384].
 - [5] N. N. Nikolaev, G. Piller and B. G. Zakharov, J. Exp. Theor. Phys. **81** (1995) 851 [Zh. Eksp. Teor. Fiz. **108** (1995) 1554] [arXiv:hep-ph/9412344]; Z. Phys. A **354**, 99 (1996) [arXiv:hep-ph/9511384].
 - [6] B. Z. Kopeliovich and A. V. Tarasov, Nucl. Phys. A **710**, 180 (2002) [arXiv:hep-ph/0205151].
 - [7] N. N. Nikolaev and B. G. Zakharov, J. Exp. Theor. Phys. **78**, 598 (1994) [Zh. Eksp. Teor. Fiz. **105**, 1117 (1994)].
 - [8] S. Gavin, P. L. McGaughey, P. V. Ruuskanen and R. Vogt, Phys. Rev. C **54**, 2606 (1996).
 - [9] K. J. Eskola, V. J. Kolhinen and R. Vogt, Nucl. Phys. A **696**, 729 (2001) [arXiv:hep-ph/0104124].

- [10] L. V. Gribov, E. M. Levin and M. G. Ryskin, Nucl. Phys. B **188**, 555 (1981); Phys. Rept. **100**, 1 (1983);
A. H. Mueller and J. w. Qiu, Nucl. Phys. B **268**, 427 (1986).
- [11] J. Raufeisen, J. C. Peng and G. C. Nayak, Phys. Rev. D **66**, 034024 (2002) [arXiv:hep-ph/0204095].
- [12] A. B. Zamolodchikov, B. Z. Kopeliovich and L. I. Lapidus, JETP Lett. **33**, 595 (1981) [Pisma Zh. Eksp. Teor. Fiz. **33**, 612 (1981)].
- [13] H. I. Miettinen and J. Pumplin, Phys. Rev. D **18**, 1696 (1978).
- [14] G. Bertsch, S. J. Brodsky, A. S. Goldhaber and J. F. Gunion, Phys. Rev. Lett. **47**, 297 (1981);
S. J. Brodsky and A. H. Mueller, Phys. Lett. B **206**, 685 (1988).
- [15] B. Blaettel, G. Baym, L. L. Frankfurt and M. Strikman, Phys. Rev. Lett. **70**, 896 (1993);
L. L. Frankfurt, A. Radyushkin and M. Strikman, Phys. Rev. D **55**, 98 (1997) [hep-ph/9610274].
- [16] V. S. Fadin and L. N. Lipatov, Phys. Lett. B **429**, 127 (1998) [arXiv:hep-ph/9802290];
M. Ciafaloni and G. Camici, Phys. Lett. B **430**, 349 (1998) [arXiv:hep-ph/9803389].
- [17] J. Bartels, K. Golec-Biernat and H. Kowalski, Phys. Rev. D **66**, 014001 (2002) [arXiv:hep-ph/0203258].
- [18] K. Golec-Biernat and M. Wüsthoff, Phys. Rev. D **59**, 014017 (1999) [hep-ph/9807513]; Phys. Rev. D **60**, 114023 (1999) [hep-ph/9903358].
- [19] M. Glück, E. Reya and A. Vogt, Eur. Phys. J. C **5**, 461 (1998) [arXiv:hep-ph/9806404].
- [20] H. Plathow-Besch, Int. J. Mod. Phys. A **10**, 2901 (1995); “PDFLIB: Proton, Pion and Photon Parton Density Functions, Parton Density Functions of the Nucleus and α_s Calculations”, User’s Manual - Version 8.04, W5051 PDFLIB, 2000.04.17, CERN-PPE.
- [21] R. Vogt, arXiv:hep-ph/0203151.
- [22] A. Donnachie and P. V. Landshoff, Phys. Lett. B **296**, 227 (1992) [arXiv:hep-ph/9209205].
- [23] K. Kodama *et al.* [Fermilab E653 Collaboration], Phys. Lett. B **263**, 573 (1991);
R. Ammar *et al.*, Phys. Rev. Lett. **61**, 2185 (1988);
M. Aguilar-Benitez *et al.* [LEBC-EHS Collaboration], Z. Phys. C **40**, 321 (1988);
G. A. Alves *et al.* [E769 Collaboration], Phys. Rev. Lett. **77**, 2388 (1996) [Erratum-ibid. **81**, 1537 (1998)];
S. Barlag *et al.* [ACCMOR Collaboration], Z. Phys. C **39**, 451 (1988).

- [24] K. Adcox *et al.* [PHENIX Collaboration], Phys. Rev. Lett. **88**, 192303 (2002) [arXiv:nucl-ex/0202002].
- [25] S. Frixione, M. L. Mangano, P. Nason and G. Ridolfi, Adv. Ser. Direct. High Energy Phys. **15**, 609 (1998) [arXiv:hep-ph/9702287].
- [26] D. M. Jansen *et al.* [E789 Collaboration], Phys. Rev. Lett. **74**, 3118 (1995).
- [27] T. Alexopoulos *et al.* [E771 Collaboration], Phys. Rev. Lett. **82**, 41 (1999).
- [28] I. Abt *et al.* [HERA-B Collaboration], arXiv:hep-ex/0205106.
- [29] R. Bonciani, S. Catani, M. L. Mangano and P. Nason, Nucl. Phys. B **529**, 424 (1998) [arXiv:hep-ph/9801375];
N. Kidonakis, E. Laenen, S. Moch and R. Vogt, Phys. Rev. D **64**, 114001 (2001) [arXiv:hep-ph/0105041].
- [30] We use standard kinematical variables, $x_2 = 2P_{Q\bar{Q}} \cdot P_1/s$ and $x_1 = 2P_{Q\bar{Q}} \cdot P_2/s$, where P_1 (P_2) is the four-momentum of the projectile (target) hadron, and $P_{Q\bar{Q}}$ is the four-momentum of the heavy quark pair. In addition, $M_{Q\bar{Q}}$ is the invariant mass of the pair, and s is the hadronic center of mass energy squared.
- [31] The Donnachie-Landshoff parameterization of the total pp cross section [22] predicts $\sigma_{\text{tot}}^{pp}(\sqrt{s} = 14 \text{ TeV}) = 100 \text{ mb}$.